Vol 15 No 6, June 2006
1009-1963/2006/15(06)/1273-05

Chinese Physics

© 2006 Chin. Phys. Soc.
and IOP Publishing Ltd

Ultraviolet and visible upconversion dynamics in Er^{3+}:$YAlO_3$ under $^2H_{11/2}$ excitation*

Yang Hai-Gui(杨海贵), Dai Zhen-Wen(戴振文)†, and Sun Zhi-Wei(孙志伟)

Department of Physics, Jilin University, Key Lab of Coherent Light, Atomic and Molecular Spectroscopy, Ministry of Education, Changchun 130023, China

(Received 22 July 2005; revised manuscript received 3 September 2005)

The luminescence of Er^{3+}:$YAlO_3$ in ultraviolet, visible and infrared ranges under the 518 nm excitation of the multiples $^2H_{11/2}$ have been investigated. Ultraviolet (275 nm and 318 nm), violet (405 nm and 413 nm) and blue (474 nm) upconversion and infrared downconversion luminescence has been observed. By means of measuring the fluorescence decay curves and using the theory of rate equations, the luminescence kinetics was studied in detail and the processes of energy transfer upconversion (ETU) and excitation state absorption (ESA) were proposed to explain the upconversion phenomena.

Keywords: ultraviolet upconversion, dynamics, Er^{3+}:$YAlO_3$
PACC: 3280K, 3220J

1. Introduction

In the last decades, because upconversion has the attractive potentiality of producing lasing emission in the visible and ultraviolet (UV) ranges,[1−4] much attention has been devoted to upconversion in rare earth (RE) ion doped crystals, glasses and fibres.[5−7] Compared to harmonic generation, upconversion needs neither stringent phase matching nor high excitation wavelength stability. Moreover, it reduces photoionization and colour-centre formation effects observed under intense UV one-photon pumping. Therefore, upconversion provides an opportunity for developing compact short-wavelength solid-state lasers.

Among all the trivalent RE ions, Er^{3+} has the richest spectra in the UV–IR range, which makes it more suited for energy upconversion studies. Visible and infrared upconversion luminescence of Er^{3+} ion has been investigated extensively in various kinds of host materials and visible upconversion laser has also been achieved in several Er^{3+}-doped materials.[5−11] UV upconversion luminescence has also been observed in several Er^{3+}-doped materials, including $Cd_{0.5}Ba_{0.3}K_{0.2}Cl_{1.8}$ and $Zn_{0.5}K_{0.5}Cl_{1.5}$ glasses, YAG, $YAlO_3$ and Cs_2NaYCl_6 crystals under $^4S_{3/2}$ excitation.[12−14] The thermalized ($^4S_{3/2}$+$^2H_{11/2}$) level provides an intermediate state for UV upconversion due to its longer lifetime.

The present paper focuses on the upconversion luminescence under 518 nm excitation of $^2H_{11/2}$ in Er^{3+}:$YAlO_3$. Several authors have reported visible upconversion luminescence in Er^{3+} doped ZBLAN, $Cs_2NaErCl_6$ and Gd_2O_3 under 514.5 nm Ar^{3+} laser excitation of $^2H_{11/2}$.[15−17] But in this work UV and visible upconversion and infrared downconversion luminescence were simultaneously observed. Compared with fluoride, although the oxide-based compound $YAlO_3$ has higher phonon energies, it is superior in mechanical hardness, thermal conductivity and optical properties. Moreover, an upconversion 550 nm laser of higher efficiency up to 13% has been realized with Er^{3+}:$YAlO_3$.[18] Therefore, upconversion investigation of Er^{3+}:$YAlO_3$ is very useful for short-wavelength laser. For the interpretation of upconversion luminescence kinetics, the decay curves of upconversion luminescence were recorded by time-resolved spectroscopy. With the help of the measured decay curves and theory of rate equations, the luminescence kinetics was studied in detail and energy transfer upconversion (ETU) and excitation state absorption

*Project supported by the National Natural Science Foundation of China (Grant No 10074020).
†E-mail address: dai@jlu.edu.cn

(ESA) were proposed to explain the upconversion phenomena. The results will be useful for realizing visible and ultraviolet upconversion lasing in Er^{3+}-doped $YAlO_3$ crystal.

2. Experiment

The dopant concentration of Er^{3+}:$YAlO_3$ crystal used in our experiment is 1at%, which was grown by the conventional Czochralski method. Its size is $1\times1\times1$ cm^3. $YAlO_3$ has a gadolinium orthoferrite structure with the orthorhombic space group D_{2h}^{16} and the Er^{3+} ions generally substitute for the Y^{3+} ions in point group symmetry C.

In our experiments the sample was excited by a dye laser (Sirah Cobra-Stretch) with coumarin 485 dye which was pumped by a frequency-tripled 355 nm Nd:YAG laser (Spectra-Physics Quanta-Ray Pro-Series) at 10 Hz repetition rate and 10 ns pulse duration. The output from the dye laser is tunable from 510 nm to 565 nm. The laser wavelength was calibrated by a pulsed wavelength meter (Burleigh WA-4500). The upconversion fluorescence was collected by a lens (f=15 cm), filtered by a 0.5 m monochromator with a resolution of 0.1 nm and finally detected by a photomultiplier tube (Hamamatsu R3896). The time-resolved fluorescence decay signals from the detector were recorded by a digital oscilloscope (Tektronix TDS 620B 500MHz) and the emission and excitation spectra were scanned with a boxcar integrator (Stanford Research Systems SR250). Each fluorescence decay curve was averaged over 100 pulses. All experiments were performed at room temperature.

3. Results and discussion

Figure 1 shows the upconversion luminescence spectrum of Er^{3+}:$YAlO_3$ under 518 nm excitation of $^2H_{11/2}$, which shows five upconversion emission bands. Based on the energy level data given by Donlan and Santiago,[19] we assign upconversion luminescence of the successive main peaks as: 275 nm ($^2H_{9/2} \rightarrow {}^4I_{15/2}$), 318 nm ($^2P_{3/2} \rightarrow {}^4I_{15/2}$), 405 nm ($^2P_{3/2} \rightarrow {}^4I_{13/2}$), 413 nm ($^2G_{9/2} \rightarrow {}^4I_{15/2}$) and 474 nm ($^2P_{3/2} \rightarrow {}^4I_{11/2}$). Figure 2 shows the excitation spectra at 275 and 405 nm upconversion luminescence. The excitation spectra are composed of two groups. One group is located between 515 and 540 nm corresponding to the resonant excitation of $^2H_{11/2}$, the other between 540 and 550 nm to that of $^4S_{3/2}$. It can be seen that the upconversion luminescence is more intense under excitation of $^2H_{11/2}$ than $^4S_{3/2}$, and the optimal excitation wavelength is 518 nm. The reason for this is that the absorption cross section of $^2H_{11/2}$ is much larger than that of $^4S_{3/2}$.[20]

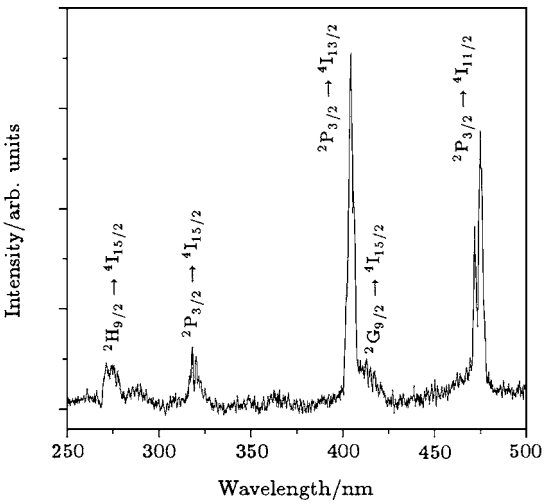


Fig.1. Upconversion luminescence spectrum under 518 nm excitation of $^2H_{11/2}$.

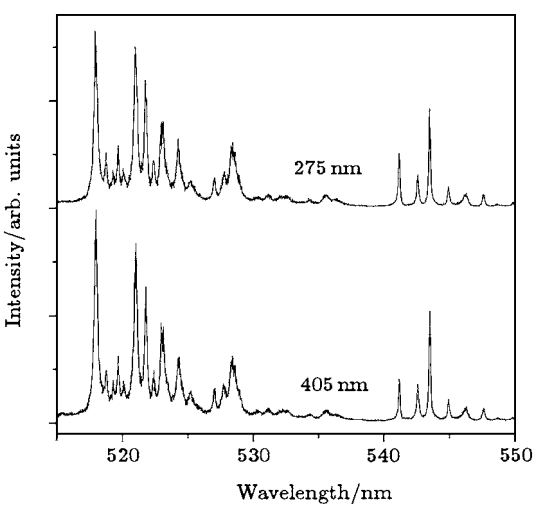


Fig.2. Excitation spectra between 515 nm and 550 nm for 275 nm and 405 nm upconversion luminescence.

The well-known upconversion mechanisms are excitation state absorption (ESA) and energy transfer upconversion (ETU). Under 514.5 nm Ar^{3+} laser excitation of $^2H_{11/2}$, violet and blue upconversion luminescence in Er^{3+}-doped ZBLAN, $Cs_2NaErCl_6$ and Gd_2O_3 has been studied according to ETU and ESA processes.[15–17] However, different from previous works, in this paper UV and visible upconversion luminescence bands emitted from higher levels were simultaneously observed under 518 nm excitation of $^2H_{11/2}$ in Er^{3+}:$YAlO_3$. Therefore, new paths lead to the upconversion luminescence in Er^{3+}:$YAlO_3$. Figure 3 gives the energy level diagram of Er^{3+} ion in

$YAlO_3$ based on the energy level data reported by Donlan and Santiago,[19] in which the possible mechanisms are shown for the observed upconversion luminescence under 518 nm excitation of the $^2H_{11/2}$ level. Here the $^2H_{11/2}$ and $^4S_{3/2}$ levels are populated due to thermal population and phonon relaxation. Through the ESA process outlined in Fig.3, the Er^{3+} ion in the $^2H_{11/2}$ state absorbs sequentially another laser photon to turn to the $^4D_{5/2}$ state, which leads to population of $^2H_{9/2}$ as well as $^2P_{3/2}$. The ETU process $^4S_{3/2} + {}^4S_{3/2} \rightarrow {}^2H_{9/2} + {}^4I_{15/2}$ populates $^2H_{9/2}$, and then from $^2H_{9/2}$ to $^2P_{3/2}$ population through multiphonon relaxation. These processes lead to upconversion luminescences around 275 nm ($^2H_{9/2}$) and 318 nm, 405 nm and 474 nm ($^2P_{3/2}$) by radiative relaxations to the lower levels $^4I_{15/2}$, $^4I_{13/2}$ and $^4I_{11/2}$, respectively. It should be pointed out that, due to the small energy gap, multiphonon relaxations from $^4D_{5/2}$ and $^2H_{9/2}$ induce the intense upconversion luminescence bands around 318 nm, 405 nm and 474 nm emitted from $^2P_{3/2}$.

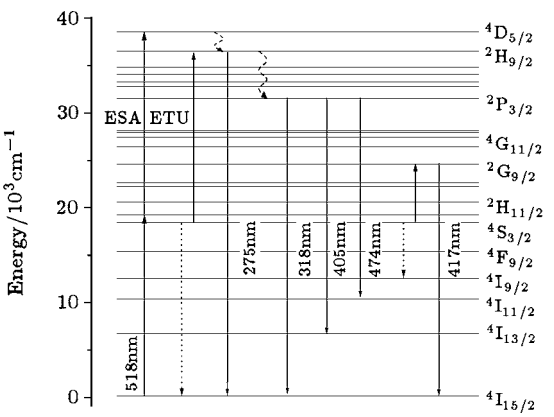


Fig.3. Energy level diagram for Er^{3+} ion showing upconversion mechanisms and emission transitions.

The time-resolved decay curves of upconversion luminescence can be used to distinguish ESA and ETU characteristics for upconversion mechanisms.[21,22] ESA process takes place during the excitation pulse, while ETU persists after the pulse for a longer period related to the lifetime of the level providing energy transfer. Therefore, upconversion decay based on ESA exhibits an exponential behaviour similar to fluorescence decay under one-photon direct excitation, while the ETU decay exhibits a rise time and a non-exponential behaviour. It can be seen from Fig.4 that a rise time containing a nearly vertical rise and a slow rise appears in upconversion luminescence decay profiles of $^2P_{3/2}$. This demonstrates that both ETU and ESA processes cause upconversion luminescence from $^2P_{3/2}$. The tail lifetime (71.5 μs) of upconversion luminescence from $^2P_{3/2}$ is longer than the real lifetime (48.7μs) of $^2P_{3/2}$, which is due to the longer lifetime 113.6μs of $^4S_{3/2}$ serving as a transmitter for the ETU process.[23]

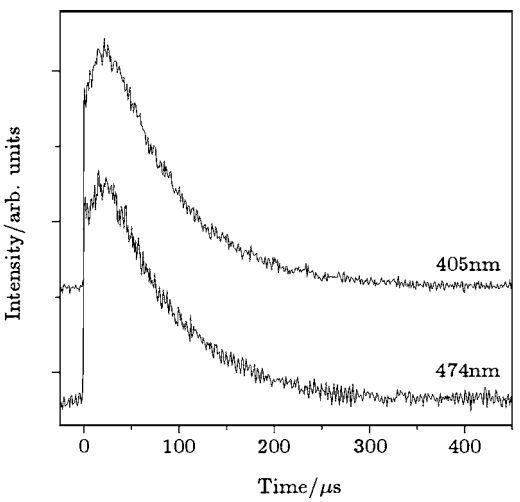


Fig.4. Decay curves of $^2P_{3/2}$ at 405 nm and 474 nm under 518 nm excitation.

The decay behaviour of upconversion luminescence is directly dependent on the lifetimes of all the levels involved. By utilizing the theory of rate equations, the decay kinetics of upconversion luminescence from $^2P_{3/2}$ was analysed. The rate equations are given as

$$\frac{dN_1}{dt} = -\frac{N_1}{\tau_1} - WN_1^2, \quad (1)$$

$$\frac{dN_2}{dt} = -\frac{N_2}{\tau_2} + \frac{1}{2}WN_1^2, \quad (2)$$

where N_1 and N_2 are the normalized population densities of $^4S_{3/2}$ and $^2P_{3/2}$, respectively. Their lifetimes $\tau_1 = 113.6\,\mu$s and $\tau_2 = 48.7\,\mu$s. W is the energy-transfer rate from $^4S_{3/2}$ to $^2H_{9/2}$, and $W = 1000\ s^{-1}$ is used in our theoretical simulations.[12] When $t = 0$, we assume $N_1 = 1$ and $N_2 = R$, where R is the initial population density of $^2P_{3/2}$, which comes from rapid multiphonon relaxation of $^4D_{5/2}$ ESA population. The theoretical decay curves are calculated in two upconversion models: only ETU (R=0) and ETU+ESA (R=0.011). It can be seen from Fig.5 that calculations with only ETU does not give a satisfactory agreement for the rise side between theory and experiment, and the theoretical rise time is longer than the measured. When both ETU and ESA are considered, a good agreement was obtained, which validates

that both ETU and ESA processes contribute to $^2P_{3/2}$ population.

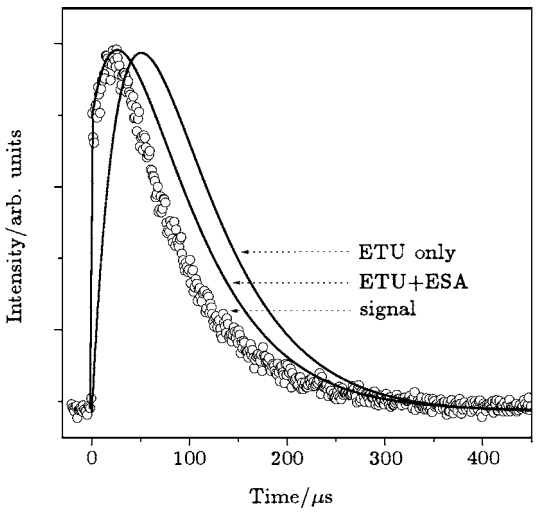


Fig.5. The measured and calculated decay curves from $^2P_{3/2}$ at 405 nm.

As seen from Fig.1, a weak upconversion emission around 413 nm was also observed. From the energy level data,[19] the energy gap of $^4S_{3/2} - {}^2G_{9/2}$ is almost equal to that of $^4I_{9/2} - {}^4S_{3/2}$. So the ETU process $^4S_{3/2}+{}^4S_{3/2} \rightarrow {}^2G_{9/2}+{}^4I_{9/2}$ is possible, and then radiation from $^2G_{9/2}$ to $^4I_{15/2}$ leads to 413 nm luminescence.

Besides upconversion luminescence, the normal luminescence spectrum of Er^{3+}:$YAlO_3$ in the region from 500 to 900 nm was obtained (see Fig.6) which shows five bands. We give the assignment of luminescence around 533 nm to the transition ($^2H_{11/2} \rightarrow {}^4I_{15/2}$), 553 nm to ($^4S_{3/2} \rightarrow {}^4I_{15/2}$), 674 nm to ($^4F_{9/2} \rightarrow {}^4I_{15/2}$), 800 nm to ($^2H_{11/2} \rightarrow {}^4I_{13/2}$) and 853 nm to ($^4S_{3/2} \rightarrow {}^4I_{13/2}$). It can be seen from Fig.7 that these five bands from thermalized ($^4S_{3/2} + {}^2H_{11/2}$) level have the same decay characters, which accords with the results by Yang *et al.*[24] The fluorescence kinetic process of $^4F_{9/2}$ consists of rise and fall periods, and its rise time is about 20 μs. From Ref.[25], we know that this kind of fluorescence reaches the maximum intensity at time $t_{\max} = \dfrac{\ln(\tau_S/\tau_F)}{1/\tau_S - 1/\tau_F}$, where $\tau_S = 113.6\,\mu$s and $\tau_F = 10.1\ \mu$s are the lifetimes of $^4S_{3/2}$ and $^4F_{9/2}$.[23] The calculated rise time $t_{\max}$= 26.8 μs is very close to the measured 20 μs. Due to multiphonon relaxation population from $^4S_{3/2}$ to $^4F_{9/2}$, the tail lifetime ($\approx 110\,\mu$s) of $^4F_{9/2}$ fluorescence is much longer than its intrinsic lifetime and shows the same decay behaviour as $^4S_{3/2}$.

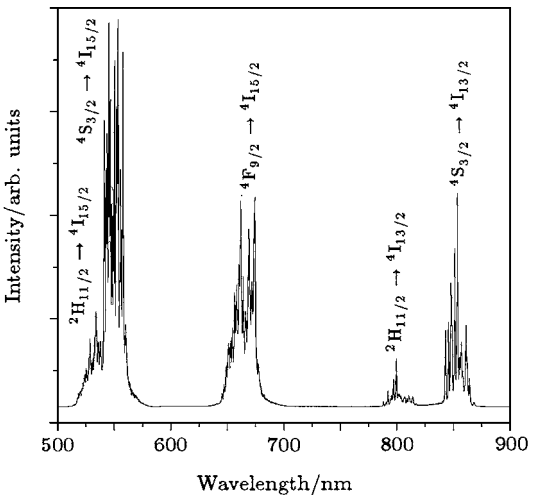


Fig.6. Luminescence spectrum in the region from 500 to 900 nm.

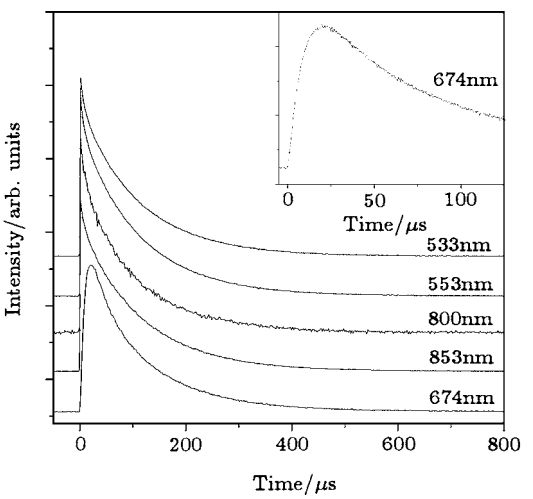


Fig.7. Decay curves from $^2H_{11/2}$, $^4S_{3/2}$ and $^4F_{9/2}$.

4. Summary

In this paper, the luminescence of ultraviolet, violet, and blue upconversion and infrared downconversion have been observed under 518 nm excitation of $^2H_{11/2}$. ESA and ETU processes bring about the population of $^4D_{5/2}$ and $^2H_{9/2}$, respectively, and the subsequent multiphonon relaxation populates $^2P_{3/2}$. By means of decay curves and rate equations, the decay kinetics of upconversion luminescence from $^2P_{3/2}$ was analysed. The conclusion is that both ETU and ESA processes contribute to the observed upconversion luminescence. Due to ETU process the decay profiles of $^2P_{3/2}$ luminescence exhibit a clear rise time and the tail lifetime is longer than the intrinsic lifetime. The fluorescence from $^2H_{11/2}$ and $^4S_{3/2}$ has the same decay, and that from $^4F_{9/2}$ exhibits a rise time of 20 μs

and its decay is almost the same as $^4S_{3/2}$ due to multiphonon relaxation from $^4S_{3/2}$ to $^4F_{9/2}$.

Acknowledgments

The authors would like to thank Professor Siyuan Zhang for providing the Er^{3+}:YAG crystal.

References

[1] Whitley T J, Millar C A, Wyatt R, Brierley M C and Szebesta D 1991 *Electron. Lett.* **27** 1785
[2] Wen L, Li S G, Huang G S, Hu L L and Jiang Z H 2004 *Chin. Phys.* **13** 0258
[3] Semashko V V, Joubert M F, Descroix E, Nicolas S, Abdulsabirov R Yu, Naumov A K, Korableva S L and Cefala A C 2000 *Proc. SPIE* **4061** 306
[4] Chen X B, Zheng Z and Song Z F 2001 *Chin. Phys.* **10** 1163
[5] Georgescu S, Toma O, Florea C and Naud C 2003*J. Lumin.* **101** 87
[6] Wang J G, Zhang Z G, Fu P M, Yan X L, W X and Jiang Y D 1998 *Acta Phys. Sin.* **47** 754 (in Chinese)
[7] Kaczmarek F, Stryla Z and Jendrzejczak A 2001 *Appl. Phys.* B **73** 125
[8] Wen L, Yang J H and H L L 2004 *Acta Phys. Sin.* **53** 4378
[9] Biswas A, Maciel G S, Friend C S and Prasad P N 2003 *J. Non-Cryst. Solids* **316** 393
[10] Tsuda M, Soga K, Inoue H, Inoue S and Makishima A 1999 *J. Appl. Phys.* **85** 29
[11] Reddy B R and Nash-Stevenson S K 1994 *J. Appl. Phys.* **76** 3896
[12] Hasan Z, Biyikli L, Sellars M J, Khodaparast G A, Richardson F S and Quagliano J R 1997 *Phys. Rev.* B **56** 4518
[13] Gharavi A and McPherson G L 1992 *Appl. Phys. Lett.* **61** 2635
[14] Xu H and Jiang Z 2002 *Phys. Rev.* B **66** 035103
[15] Tanner P A 1988 *Molec. Phys.* **63** 365
[16] Gan F, Wang J and Chen Y 1997 *J. Non-Cryst. Solids* **213**&**214** 261
[17] Guo H, Li Y, Wang D, Zhang W, Yin M, Lou L and Xia S 2004 *J. Alloys Compounds* **376** 23
[18] Scheps R 1994 *IEEE J. Quantum Electron.* **30** 2914
[19] Donlan V E and Santiago A A 1972 *J. Chem. Phys.* **57** 4717
[20] Yu Y, Wu Z and Zhang S 2000 *J. Alloys Compounds* **302** 204
[21] Hehlen M P, Frei G and Güdel H U 1994 *Phys. Rev.* B **50** 16264
[22] Riedener T, Egger P, Hulliger J and Güdel H U 1997 *Phys. Rev.* B **56** 1800
[23] Xu H, Zhou L, Dai Z and Jiang Z 2002 *Physica* B **324** 43
[24] Yang Z, Huang S, Lü S and Chen B 2004 *J. Non-Cryst. Solids* **343** 154
[25] Weber M J 1973 *Phys. Rev.* B **8** 54